

Low-temperature Structures and Raman Spectra of Crystalline Modifications of Selenium Difluoride Dioxide†

Alexander J. Blake,^{*a} Danila Bevilacqua,^a Miloš Černík^b and Zdirad Žák^b

^a Department of Chemistry, The University of Edinburgh, West Mains Road, Edinburgh EH9 3JJ, UK

^b Department of Inorganic Chemistry, Masaryk University, Kotlářská 2, 611 37 Brno, Czech Republic

Low-temperature Raman spectra of solid SeO_2F_2 indicated the existence of two crystalline modifications between 174 and 100 K, the crystal and molecular structures of which have been determined by single-crystal X-ray diffraction techniques at 150 and 120 K. At about 130 K the higher-temperature tetragonal α form undergoes a first-order phase transformation to give the lower-temperature monoclinic β form. In both modifications the SeO_2F_2 molecules have similar distorted tetrahedral geometries: the weighted averages of the bond parameters are Se–O 1.57(1), Se–F 1.66(1) Å, O–Se–O 126.7(9), F–Se–F 94(2) and O–Se–F 107.9(2)°. The molecules are only very weakly associated through intermolecular Se–O...Se contacts: in the α form each selenium atom is co-ordinated by two oxygen atoms from two different neighbouring molecules, while the oxygen atoms have contacts to two other molecules forming a three-dimensional network. In the β form these Se–O...Se contacts give rise to a structure consisting of corrugated layers of SeO_2F_2 molecules. Raman spectra of both modifications are consistent with their crystal structures and a factor-group correlation analysis confirmed the observed splittings of the Se–F stretching modes.

Selenium difluoride dioxide is a gas under normal conditions, liquifying at 265 K and freezing as colourless crystals at 174 K.¹ The Raman spectrum^{2,3} of liquid SeO_2F_2 and its gas-phase IR spectrum³ were assigned assuming C_{2v} molecular symmetry and a normal coordinate analysis was carried out using either Urey–Bradley⁴ or modified general valence force fields.^{5,6} A distorted-tetrahedral shape for the SeO_2F_2 molecule was later confirmed by an electron-diffraction study.⁷

In contrast to the chemically almost inert SO_2F_2 , SeO_2F_2 is a highly reactive compound and this difference may be rationalised in terms of a number of factors:^{1,8} the high oxidising power of selenium(vi); the greater polarity of Se–O and Se–F bonds compared with S–O and S–F bonds; and to the unsaturated co-ordination of the selenium atom. The unsaturation is manifested in the ability of the Se atom in SeO_2F_2 and in other selenonyl compounds to act as an electron-pair acceptor. This Lewis acidity of SeO_2XY molecules is reflected in the formation of more or less stable 1:1 donor–acceptor complexes with some nitrogen- and oxygen-containing donor molecules.⁹ Although no direct structural information is available on these complexes, the marked decrease in all Se–O and Se–F stretching frequencies by some 60–150 cm^{-1} indicates the formation of a relatively strong D \rightarrow Se donor–acceptor bond.

On the other hand, the Se=O double bonds in an SeO_2 group display very low basicity, so that almost no complexes of selenonyl compounds with Lewis acids are known. Actually, only the formation of weak oxygen-bridged molecular complexes of the form $(\text{SbF}_5)_n \cdot \text{SeO}_2\text{F}_2$ ($n = 1-5$)¹⁰ has been reported, whereas the ¹⁹F NMR spectrum indicated the absence of complex formation between SeO_2F_2 and AsF_5 down to 193 K.¹¹

Therefore, despite the evident Lewis acidity of SeO_2F_2 with strong Lewis bases, the marked inability of its oxygen atoms to act as an electron-pair donor would predict only a slight tendency to self-association in the condensed states.

However, a relatively high value (107.0 $\text{J K}^{-1} \text{mol}^{-1}$) for the entropy of vapourisation (Trouton constant) of SeO_2F_2 ¹ implies some association even in the liquid phase. Establishing the nature of the intermolecular association in the solid state would obviously help to understand better the bonding and chemical reactivity of this molecule.

Raman spectra of solid SeO_2F_2 showed only slight frequency shifts in Se–O and Se–F stretching modes compared with the liquid but the observed temperature dependence of spectral band splittings indicated the probable existence of two distinct crystalline modifications. We have succeeded in growing single crystals of both phases *in situ* on a diffractometer and determining their structures.

Experimental

Selenium difluoride dioxide was prepared by the reaction of HSO_3F with anhydrous selenic acid¹² and purified by repeated vacuum distillation on a Pyrex vacuum line equipped with greaseless stopcocks. Its ¹⁹F NMR spectrum¹³ did not reveal any fluorine-containing impurities. Samples for Raman and X-ray structure analysis were condensed and sealed into Pyrex capillaries of appropriate diameters.

Raman Spectroscopy.—Raman spectra were recorded on a Spex Ramalog 3 spectrometer equipped with Spectra-Physics model 165 argon-ion laser using the 488 nm line and output power of 200–400 mW. The low-temperature Raman spectra were obtained at 160 and 120 K using 90° scattering geometry in a variable-temperature quartz cell described by Miller and Harney.¹⁴ Spectra were calibrated using argon-ion emission lines and reported frequencies should be accurate within $\pm 2 \text{ cm}^{-1}$.

Crystal Structure Determination.—The capillary containing condensed SeO_2F_2 was mounted in a thermally insulating Tufnol tip and transferred on a goniometer head to a Stoe Stadi-4 four-circle diffractometer equipped with an Oxford Cryosystems low-temperature device.¹⁵ A single crystal of each phase was prepared by converting a polycrystalline sample into

† Supplementary data available: see Instructions for Authors, *J. Chem. Soc., Dalton Trans.*, 1995, Issue 1, pp. xxv–xxx.

a single crystal using miniature zone-melting techniques,¹⁶ at 170 K for the higher-temperature α phase and at 120 K for the lower-temperature β phase. These methods allowed us to obtain crystals of the β form directly from the liquid, thereby by-passing the phase boundary between the two solid forms.

For each phase, diffraction amplitudes were collected using ω - 2θ scans with ω scan width of $(0.99 + 0.346 \tan \theta)^\circ$. The stability of the crystal was monitored using three standard reflections and no significant crystal decay or movement was observed. The intensities were converted into squared structure amplitudes by applying Lorentz-polarisation and semi-empirical absorption corrections. The crystal data and selected experimental details are summarised in Table 1. The following programs were used: SHELXS 86¹⁷ for structure solution, SHELXL 93¹⁸ for structure refinement on F^2 and molecular geometry calculations, and PLUTO¹⁹ to prepare the illustrations. Atomic scattering factors were those as inlaid in SHELXL 93. The final atomic coordinates are given in Table 2.

Additional material available from the Fachinformationszentrum Karlsruhe comprises thermal parameters and remaining bond lengths and angles.

Results and Discussion

Structures of α -SeO₂F₂ and β -SeO₂F₂.—In both phases SeO₂F₂ molecules exhibit distorted-tetrahedral geometries which differ only slightly from that seen in the gas phase. The bond lengths, valence angles and some important intermolecular contacts are listed in Table 3.

The tetragonal α modification is isostructural with its sulfur analogue SO₂F₂.²⁰ Fig. 1 shows a projection of the structure approximately along the crystallographic c axis. Apart from its primary O₂F₂ co-ordination, each Se atom participates in two weak, symmetry related contacts to oxygen atoms in different adjacent molecules: at 3.20 Å these are slightly less than the sum of the van der Waals radii for Se and O atoms (3.4 Å²¹). Both

oxygen atoms in each molecule are therefore involved in these Se—O...Se contacts which lie approximately *trans* to the fluorine atoms (F—Se...O 175.3°) giving, overall, a strongly distorted octahedral environment around each selenium atom. As a consequence, each molecule is bound to its four nearest neighbours forming a three-dimensional network as can be seen in Fig. 1.

The structure of the monoclinic β form differs solely in the disposition of these intermolecular contacts, the intramolecular parameters being virtually the same in both modifications. Fig. 2 shows the projection approximately down the crystallographic a axis. There are two independent molecules in the asymmetric unit of the β modification which exhibit slightly different Se—O...Se intermolecular contacts, 3.10 and 3.15 Å for molecule 1 and 3.13 and 3.22 Å for molecule 2. Again, every

Table 2 Atomic coordinates ($\times 10^4$)

Atom	<i>x</i>	<i>y</i>	<i>z</i>
α -SeO ₂ F ₂			
Se	908(2)	908(2)	0
F	-1 302(11)	296(15)	959(9)
O	3 369(11)	290(13)	636(6)
β -SeO ₂ F ₂			
Se(1)	8 423(4)	908(2)	2 165(3)
F(11)	9 072(4)	-120(9)	1 662(19)
F(12)	10 676(25)	1 366(9)	1 440(17)
O(11)	5 944(27)	1 183(11)	846(20)
O(12)	9 111(33)	986(11)	4 254(21)
Se(2)	5 520(4)	3 588(2)	1 792(3)
F(21)	3 071(21)	3 150(9)	2 364(18)
F(22)	4 435(24)	3 300(9)	-328(18)
O(21)	5 381(25)	4 626(11)	1 879(20)
O(22)	7 791(26)	2 983(10)	2 593(21)

Table 3 Bond lengths (Å) and interatomic angles (°) in α - and β -SeO₂F₂

α -SeO ₂ F ₂			
Se—O	1.563(6)	O—Se—O ⁱ	125.5(5)
Se—F	1.650(7)	F—Se—O	107.9(4)
		F—Se—O ⁱ	107.5(4)
		F—Se—F ⁱ	96.6(7)
Next-nearest contacts			
Se—O ⁱⁱ	3.200(7)	O ⁱⁱⁱ —Se—O ⁱⁱⁱ	103.4(3)
Se—O ⁱⁱⁱ	3.200(7)	Fe—Se—O ⁱⁱⁱ	175.3(3)
		Se—O ⁱⁱ —Se ⁱⁱ	124.5(5)
β -SeO ₂ F ₂			
Se(1)—O(11)	1.57(1)	Se(2)—O(21)	1.55(2)
Se(1)—O(12)	1.58(2)	Se(2)—O(22)	1.57(2)
Se(1)—F(11)	1.65(1)	Se(2)—F(21)	1.68(1)
Se(1)—F(12)	1.66(1)	Se(2)—F(22)	1.67(1)
O(11)—Se(1)—O(12)	127.4(9)	O(21)—Se(2)—O(22)	127.1(7)
O(11)—Se(1)—F(11)	107.5(8)	O(21)—Se(2)—F(21)	108.8(7)
O(11)—Se(1)—F(12)	107.5(8)	O(21)—Se(2)—F(22)	106.9(7)
O(12)—Se(1)—F(11)	107.6(8)	O(22)—Se(2)—F(21)	108.2(7)
O(12)—Se(1)—F(12)	107.8(8)	O(22)—Se(2)—F(22)	108.0(8)
F(11)—Se(1)—F(12)	94.0(7)	F(21)—Se(2)—F(22)	92.2(7)
Next-nearest contacts			
Se(1)—O(21 ⁱ)	3.10(2)	Se(2)—O(11 ⁱⁱ)	3.13(2)
Se(1)—O(22)	3.15(2)	Se(2)—O(12 ⁱⁱⁱ)	3.22(2)
F(11)—Se(1)—O(22)	168.6(6)	F(21)—Se(2)—O(12 ⁱⁱⁱ)	156.7(5)
F(12)—Se(1)—O(21 ⁱ)	165.8(6)	F(22)—Se(2)—O(11 ⁱⁱ)	161.0(6)
O(21 ⁱ)—Se(1)—O(22)	118.7(4)	O(11 ⁱⁱ)—Se(2)—O(12 ⁱⁱⁱ)	134.1(4)
Se(1)—O(22)—Se(2)	129.0(7)		

Symmetry codes for α -SeO₂F₂: i *y*, *x*, -*z*; ii 0.5 - *x*, 0.5 + *y*, 0.25 - *z*; iii 0.5 + *y*, 0.5 - *x*, *z* - 0.25. Symmetry codes for β -SeO₂F₂: i 1 - *x*, *y* - 0.5, 0.5 - *z*; ii *x*, 0.5 - *y*, 0.5 + *z*; iii *x*, 0.5 - *y*, *z* - 0.5.

Table 1 Crystal data and structure refinement

	α -SeO ₂ F ₂	β -SeO ₂ F ₂
Formula	F ₂ O ₂ Se	F ₂ O ₂ Se
<i>M</i>	148.96	148.96
<i>T</i> /K	150(2)	120(2)
λ /Å	0.710 73	0.710 73
System	Tetragonal	Monoclinic
Space group	<i>P</i> 4 ₁ 2 ₁ 2	<i>P</i> 2 ₁ / <i>c</i>
<i>a</i> /Å	5.495(9)	5.634(5)
<i>b</i> /Å	5.495(9)	14.94(2)
<i>c</i> /Å	11.10(2)	7.803(7)
α /°	90	90
β /°	90	104.23(8)
γ /°	90	90
<i>U</i> /Å ³	335.2(9)	636.5(10)
<i>Z</i>	4	8
<i>F</i> (000)	272	544
<i>D</i> _c /Mg m ⁻³	2.951	3.109
μ /mm ⁻¹	11.071	11.662
2 θ Range/°	8.28–59.80	5.46–45.04
Reflections collected	507	827
Independent reflections	487	827
<i>R</i> (int)		0.0327
Refinement method	Full-matrix least squares on <i>F</i> ²	
Data/parameters	484/24	822/92
<i>S</i> on <i>F</i> ²	1.078	1.044
<i>R</i> 1 [<i>F</i> > 4 σ (<i>F</i>), all]	0.0464, 0.0764	0.0884, 0.1423
<i>wR</i> 2 [<i>I</i> > 2 σ (<i>I</i>), all]	0.1130, 0.1323	0.2451, 0.3150
Extinction coefficient		0.009(5)
$\Delta\rho_{\max}$, $\Delta\rho_{\min}$ /e Å ⁻³	0.964, -0.659	2.558, -1.544

$R1 = \sum |F_o| - |F_c| / \sum |F_o|$; $wR2 = [\sum w(F_o^2 - F_c^2)^2 / \sum wF_o^4]^{1/2}$; $w = 1 / [\sigma^2(F_o^2) + aP^2 + bP]$, where $P = 0.333[\max. \text{ of } (0 \text{ or } F_o^2)] + 0.667F_c^2$.

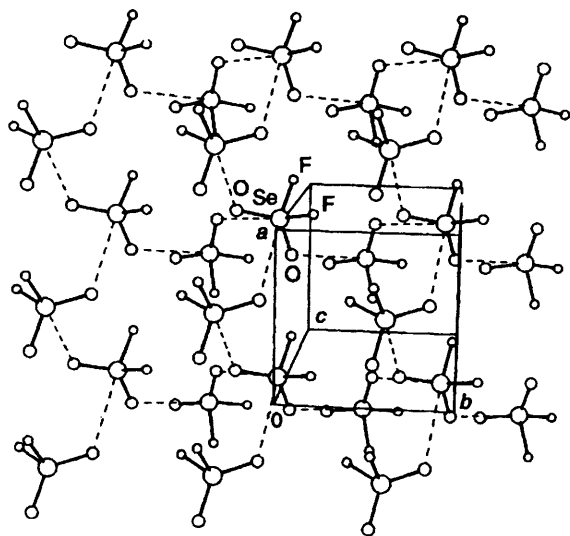


Fig. 1 The three-dimensional network in the structure of α - SeO_2F_2 . This view is approximately along the c axis

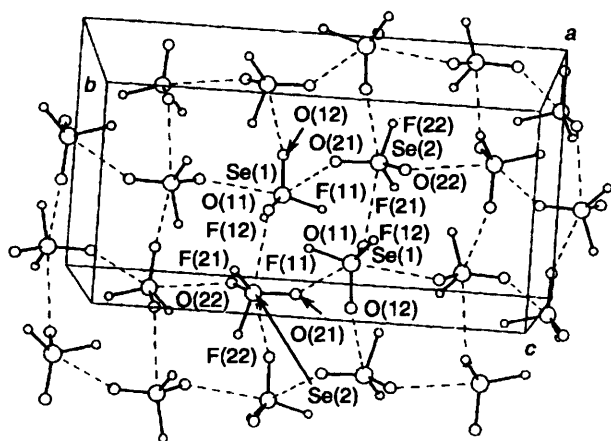


Fig. 2 Part of one two-dimensional sheet in the structure of β - SeO_2F_2 . This view is approximately along the a axis

molecule is linked *via* $\text{Se-O}\cdots\text{Se}$ interactions to its four nearest neighbours but in contrast to α - SeO_2F_2 , the intermolecular bridging gives rise to a structure consisting of two-dimensional corrugated layers parallel to (100), with no apparent contacts between adjacent layers.

Raman Spectra.—In principle, the comparison of Raman spectra from the different phases of SeO_2F_2 should yield some information about the nature of its association in the condensed states. The stretching frequencies of the bonds formed by the atoms involved in the intermolecular bridging should decrease when going from the gas to the liquid or crystalline solid. On the other hand, the bonds of the atoms not involved in bridging should show no decrease or, more probably, a small increase in frequency.

The effect of molecular self-association upon the stretching frequencies of the bonds involved can be observed, for example, in the Raman spectra of seleninyl dichloride^{22,23} and difluoride.^{23,24} Monomeric molecules have been found in the vapour, while there is spectroscopic evidence for some degree of association in the liquid state and relatively strong intermolecular interactions in the solid phase. To illustrate this tendency, the corresponding frequency shifts of all three stretching vibrations of SeOF_2 are given in Table 4. On going from the gas to the solid, there is an appreciable decrease in $\nu(\text{SeO})$, whereas the corresponding increase in both SeF

Table 4 Frequencies (cm^{-1}) of stretching vibrations of gaseous (393 K), liquid, and solid SeOF_2 ²⁴

Vibrations	Gas	Liquid	Solid
$\nu(\text{SeO})$	1049	1007	956 + 968 + 979
$\nu_{\text{sym}}(\text{SeF}_2)$	667	658	648 + 658 + 698
$\nu_{\text{asym}}(\text{SeF}_2)$	637	603	610 + 622

stretching modes is not so pronounced. This is obviously related to the simultaneous presence of both $\text{Se-O}\cdots\text{Se}$ and $\text{Se-F}\cdots\text{Se}$ bridges in the structure of crystalline seleninyl difluoride.²⁵

In contrast, the Se-F bonds in fluoride oxides of Se^{VI} are not involved in any $\text{Se-F}\cdots\text{Se}$ bridging, as can be seen in SeOF_4 which dimerises to $\text{Se}_2\text{O}_2\text{F}_8$ *via* Se-O-Se bridges only.¹³ Furthermore, the Se=O bonds in SeO_2F_2 have lower basicity in comparison with that in SeOF_2 and, consequently, in a condensed state SeO_2F_2 molecules interact with their neighbours only very weakly, and only relatively small frequency shifts of the stretching modes of all bonds involved can be expected.

The negligible differences between frequencies of the ν_1, ν_2, ν_6 and ν_8 fundamentals in the IR spectrum of gaseous³ and the Raman spectrum of liquid SeO_2F_2 ^{2,3} correspond well with this prediction. Unfortunately, the Raman spectra of the gas-phase or matrix-isolated SeO_2F_2 do not appear to have been reported, so that there is no opportunity for a direct comparison of Raman spectra in different phases. We therefore recorded the Raman spectrum of a CCl_3F solution (9.6 wt%) but the frequencies of the ν_1, ν_2 and ν_8 (ν_6 is obscured by a band of the solvent) stretching modes (Table 5) are within experimental errors virtually the same as in the pure liquid. Thus, notwithstanding the reported higher value of the Trouton constant,¹ no intermolecular association could be proved by vibrational spectroscopy in liquid SeO_2F_2 .

The observed Raman frequencies of both modifications of solid SeO_2F_2 are listed and assigned in Table 5 and compared with the spectra of liquid SeO_2F_2 and its CCl_3F solution. Although nine Raman-active fundamentals are expected for the SeO_2F_2 molecule with C_{2v} symmetry, as a result of partial overlap only six bands are actually observed in the spectrum of the liquid.² In the spectra of both solid phases most bands are split into several components which in part also overlap and, consequently, it is difficult to determine their original frequencies. This occurs especially in the region of the ν_3, ν_5, ν_7 and ν_9 fundamentals ($330\text{--}370\text{ cm}^{-1}$), so that the entire spectrum consists of five groups of split bands only: ν_1, ν_2 and ν_8, ν_4, ν_6 , and the four remaining fundamentals mentioned above.

The best resolved group of bands corresponds to the two SeF stretching modes ν_2 and ν_8 , extending over a range of $20\text{--}30\text{ cm}^{-1}$ and displaying quite distinct appearances in α - and β - SeO_2F_2 (Fig. 3). To account for the observed splittings, a factor-group analysis has been performed. From the structural point of view, there are no ambiguities in either modification. In the tetragonal α form there are four molecules *per* unit cell, each on a site of C_2 symmetry, whereas eight SeO_2F_2 molecules are situated on two separate sets of four-fold general positions in the monoclinic β modification. The correlations of free molecule symmetry C_{2v} with corresponding site and factor groups for both modifications are given in Fig. 4.* Only the SeF stretching modes, ν_2 and ν_8 , which show sufficiently large and well resolved splittings, were considered. The orientation of the site group C_2 within the unit cell in the case of the space group $P4_12_12 \equiv D_4^2$ (no. 92) was chosen according to Boyle²⁶ as $C_2 \rightarrow C_2'$.

* As no translatory or rotatory modes were observed in the spectra, these have been omitted from the correlation diagram for clarity.

Table 5 Raman frequencies (cm^{-1}) of liquid and solid SeO_2F_2

Liquid ²	Solution* in CFCl_3	Solid		Assignment ⁵
		α form	β form	
1059w		1050w	1054w	$\nu_6(\text{B}_1)$
971vs	970	969 (sh)	971m	$\nu_1(\text{A}_1)$
		966vs	965vs	
		734w		
		724w	722w	$\nu_2(\text{A}_1)$
		714w	715s	
		707vs	709m	$\nu_8(\text{B}_2)$
702vs	700	702 (sh)	699m	
		371 (sh)	370m	
360m		367m	359w	$\nu_3(\text{A}_1)$
		354w	355m	
		347w		$\nu_5(\text{A}_2)$
340w		341vw		
		333vw		$\nu_7(\text{B}_1)$
			292w	$\nu_4(\text{A}_1)$
			289w	
277m		285m	278m	
		281m		

* Concentration 9.6 wt%; other fundamentals are obscured by solvent bands.

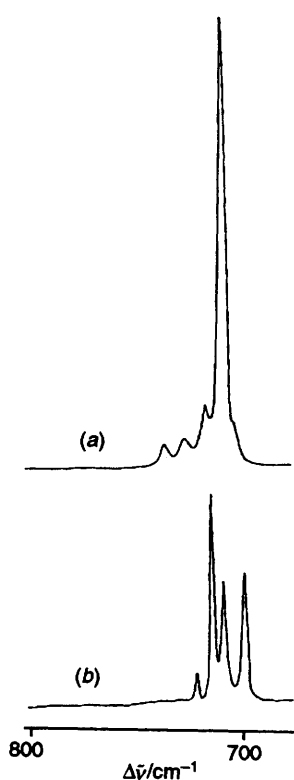


Fig. 3 Raman spectra of α - SeO_2F_2 at 160 K (a) and β - SeO_2F_2 at 120 K (b) in the ν_2 and ν_8 regions

As follows from the correlation diagrams, the $3\nu_2$ and $2\nu_8$ fundamentals should be Raman-active in the vibrational spectra of the higher-temperature α form, whereas $4\nu_2$ and $4\nu_8$ should be expected in the Raman spectrum of the lower-temperature β - SeO_2F_2 . The agreement with the selection rules is excellent for the former, while only four bands were observed in the $\nu(\text{SeF})$ region (699 – 722 cm^{-1}) in the spectrum of the latter. This represents only one half of the predicted number and can probably be attributed either to an accidental degeneracy of the ν_2 and ν_8 modes arising from two distinct four-fold sets of SeO_2F_2 molecules occupying equivalent points with the C_1 site symmetry or to insufficient spectral resolution respectively.

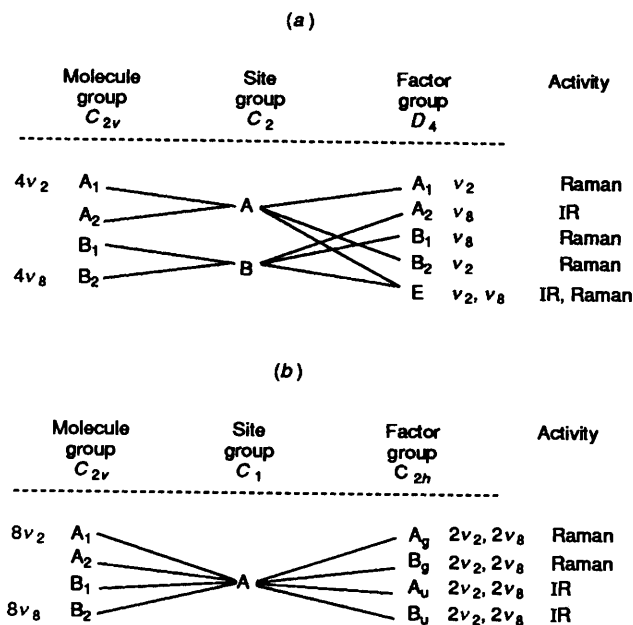


Fig. 4 Correlation diagrams and selection rules for α - SeO_2F_2 (a) and β - SeO_2F_2 (b)

Comparison between the Raman spectra of solid and liquid SeO_2F_2 reveals that, as expected, in the former the average frequencies of SeO stretching modes are slightly shifted downwards and those of SeF stretching upwards from the corresponding frequencies of the latter. These shifts can be attributed to a certain bifunctional behaviour of SeO_2F_2 , which acts as an electron-pair donor *via* the oxygen atoms and, simultaneously, as an electron-pair acceptor through the selenium atom. In that way a spatially oriented weak association of SeO_2F_2 molecules occurs *via* $\text{Se}-\text{O}\cdots\text{Se}$ bridges and either a three-dimensional network or two-dimensional sheet structure is formed, as has been found in the crystal structures of the α - and β -modifications.

Acknowledgements

Z. Ž. expresses his appreciation to the European Community's Tempus Scheme, contract no. IMG-CZT-0140-90, for financial support. He also thanks the Department of Chemistry, The University of Edinburgh, for the use of facilities.

References

- 1 A. Engelbrecht and B. Stoll, *Z. Anorg. Allg. Chem.*, 1957, **292**, 20.
- 2 R. Paetzold and K.-H. Ziegenbalg, *Z. Chem.*, 1964, **4**, 461.
- 3 T. Birchall and R. J. Gillespie, *Spectrochim. Acta*, 1966, **22**, 681.
- 4 K. Ramaswamy and S. Jayaraman, *J. Mol. Struct.*, 1970, **5**, 325.
- 5 J. Toužin and I. Horsák, *Spisy Přírodověd. Fak. Univ. J. E. Purkyně Brno*, 1969, **499**, 7; *Chem. Abstr.*, 1979, **74**, 79958.
- 6 S. Mohan and S. Srinivasan, *J. Indian Chem. Soc.*, 1987, **64**, 530.
- 7 K. Hagen, V. R. Cross and K. Hedberg, *J. Mol. Struct.*, 1978, **44**, 187.
- 8 R. Paetzold, *Z. Chem.*, 1964, **4**, 321.
- 9 R. Kurze and R. Paetzold, *Z. Anorg. Allg. Chem.*, 1972, **387**, 361.
- 10 R. J. Gillespie and M. Parekh, Abstracts of the 4th International Conference on Non-Aqueous Solutions, Vienna, 1974, p. 43.
- 11 M. Černík, unpublished work.
- 12 K. Seppelt, *Chem. Ber.*, 1972, **105**, 2431.
- 13 K. Seppelt, *Z. Anorg. Allg. Chem.*, 1974, **406**, 287.
- 14 F. A. Miller and B. M. Harney, *Appl. Spectroscopy*, 1970, **24**, 271.
- 15 J. Cosier and A. M. Glazer, *J. Appl. Crystallogr.*, 1986, **19**, 105.
- 16 B. J. McArdle and J. N. Sherwood, in *Advanced Crystal Growth*, eds. P. M. Dryburgh, B. Cockayne and K. G. Barraclough, Prentice Hall, London, 1987, pp. 183, 184.
- 17 G. M. Sheldrick, *Acta Crystallogr., Sect. A*, 1990, **46**, 467.
- 18 G. M. Sheldrick, SHELXL 93, University of Göttingen, 1993.

- 19 W. D. S. Motherwell, PLUTO, program for plotting crystal and molecular structures, University of Cambridge, 1976.
- 20 D. Mootz and A. Merschenz-Quack, *Acta Crystallogr., Sect. C*, 1988, **44**, 924.
- 21 L. Pauling, *The Nature of the Chemical Bond*, 3rd edn., Oxford University Press, London, 1960.
- 22 W. Bues, W. Brockner and F. Demiray, *Z. Anorg. Allg. Chem.*, 1977, **434**, 249.
- 23 J. Milne, *Spectrochim. Acta, Ser A*, 1982, **38**, 569.
- 24 L. E. Alexander and I. R. Beattie, *J. Chem. Soc., Dalton Trans.*, 1972, 1745.
- 25 J. C. Dewan and A. J. Edwards, *J. Chem. Soc., Dalton Trans.*, 1976, 2433.
- 26 L. L. Boyle, *Acta Crystallogr., Sect. A*, 1971, **27**, 76.

Received 21st September 1994; Paper 4/05753H